# USE OF EDI TIME-OF-FLIGHT DATA FOR FGM CALIBRATION CHECK ON CLUSTER

**E. Georgescu[(1)], H. Vaith[(1)], K-H. Fornacon[(2)], U. Auster[(2)], A. Balogh[(3)], C. Carr[(3)], M. Chutter[(4)], M. Dunlop[(5)], M. Foerster[(1)], K-H. Glassmeier[(2)], J. Gloag[(3)], G. Paschmann[(1)], J. Quinn[(4)] and R.Torbert[(4)]**

*[(1)] Max-Planck Institute for Extraterrestrial Physics, Garching, Germany, Email: eg@mpe.mpg.de*
*[(2)] Institute for Geology and Extraterrestrial Physics, Technical University Braunschweig, Germany*
*[(3)] Imperial College London, UK*
*[(4)] University of New Hampshire, Durham, USA*
*[(5)] Rutherford Appleton Laboratory, Didcot, UK*

## ABSTRACT

The four Cluster satellites launched in summer 2000 carry flux-gate magnetometers (FGM), which measure the magnetic field vector. The satellites also carry electron drift instruments (EDI) that measure the gyration time of electrons perpendicular to the magnetic field. The gyration time is related through a universal constant to the magnetic field magnitude and is hence an absolute measure of it. The knowledge of the field magnitude can be used to verify the magnetometer calibration or to carry out a scalar calibration of FGM, similarly to near-Earth space missions where proton magnetometers provide this information. The resulting increased accuracy of the magnetic field measurement on the four spacecraft enhances the value of the multipoint measurements on Cluster by reducing the uncertainties in deriving the differential quantities such as the curl of the magnetic field.

In this paper the errors in the measurements made by FGM and EDI are discussed and a comparison of the measurements is presented. The conclusion is that the absolute error of the magnetic field measurement is about 0.1 nT for fields below 100 nT and less than 0.1% for fields above.

## 1. INTRODUCTION

### 1.1 Context of Observation

The four spacecraft of the Cluster mission, flying in a tetrahedral formation in an eccentric polar orbit, carry identical sets of fields-and-particles instruments. The separation between spacecraft in the tetrahedral configuration varies between ~100 km and (as planned for later stages in the mission) ~10,000 km. Qualitative and quantitative intercomparison between measurements made on the four spacecraft are used to characterise the plasma phenomena and structures encountered by Cluster in three-dimensions, and to separate, on the scale of the interspacecraft separation distances, temporal and spatial effects. However, this objective can only be reached if the instruments on the four spacecraft are intercalibrated in such a way that differences measured between spacecraft have a high accuracy.

Given the importance of the measurements of the magnetic field in space plasmas in general, and on Cluster in particular for the derivation of current densities, the determination of wave vectors and the geometry and dynamics of plasma boundaries, the absolute calibration of the magnetometers is an important objective. Space missions, exploring the inner magnetosphere, like, recently, CHAMP (see [3] or: *http://op.gfz-potsdam.de/champ/index_CHAMP.html*) and Oersted (see [4] or the instrument web-page: *http://web.dmi.dk/projects/oersted/mission/instruments.html*), are equipped for the in-flight calibration with proton magnetometers, which measure the field magnitude absolutely, but only in fields above 10000 nT The Cassini experiment: has on board a Vector/Scalar Helium-Magnetometer operating in magnetic fields up to 256 nT *(http://www.sp.ph.ic.ac.uk/cassini/vshm.html).*

The Electron Drift Instrument, first time operated successfully on Equator-S is able to measure the magnetic field magnitude down to 20 nT. The short lifetime of the spacecraft did not offer a large enough statistics of EDI time-of-flight data, such that a thorough comparison of the magnetic field measurements was not possible. An estimation of the spacecraft spin axis offset was still performed ([5], [6]).

In case of CLUSTER, EDI is working successfully since the beginning of the mission allowing for the characterization of the instrument as a scalar magnetometer. Thanks to the presence of EDI, the calibration of the vector magnetometer (FGM) can be verified and a higher accuracy achieved than on previous magnetospheric missions.

Following the brief description of the relevant aspects of the two instruments in the Cluster payload, we describe the methodology of the comparison of the measurements and give the outcome of the intercalibration process.

### 1.2 Instrument overview: FGM

The four Cluster spacecrafts carry identical instruments to measure the magnetic field. Each instrument, in turn, consists of two triaxial fluxgate magnetometers and an on-board Data-Processing Unit (DPU).

The fluxgate magnetometers are similar to many previous instruments flown in Earth-orbit and on other, planetary and interplanetary missions. For more details and technical characteristics, see [1] or the instrument home page:
*http://www.sp.ph.ic.ac.uk/Cluster/instrov.html*

One of the magnetometer sensors (the outboard, or OB sensor) is located at the end of one of the two 5.2 m radial booms in order to minimize the influence of the spacecraft background field at the location of the sensor and is used most of the time as Primary sensor. The other (the inboard, or IB sensor) is located 1.5 m inward and it is mostly used as Secondary and acquires data at much lower rate. The magnetometers have eight possible operating ranges; of these, five are used on the Cluster magnetometers, shown in Table 1. These ranges were selected to provide good resolution in the solar wind (where the magnitude of the field is typically between 3 and 30 nT), and up to the highest field values expected in the magnetosphere along the Cluster orbit (up to about 1,000 nT). The highest range ( 65,500 nT) was used only to facilitate ground testing. Range selection can be automatic (controlled by the instrument DPU) or commanded from the ground. When in the automatic mode, a range selection algorithm, running in the DPU continuously, monitors each component of the measured field vector. If any component exceeds a fraction (set at 90 %) of the range, an up-range command is generated and transmitted to the magnetometer. If all three components are smaller than 10 % of the range for more than a complete spin period (in fact for more than the telemetry frame period of 5.15222 s), an automatic down-range command is generated to the magnetometer. The digital resolution, corresponding to the five ranges of the magnetometers, is shown in Table 1.

Table 1. Digital resolution of FGM

| Range (nT) | Digital Resolution (nT) |
|---|---|
| -64 to +63.992 | 7.813 x 10-3 |
| -256 to +255.97 | 3.125 x 10-2 |
| -1024 to +1023.9 | 0.125 |
| -4096..+4095.5 | 0.5 |
| -65536..+65528 | 8 |

The data-acquisition process is controlled by the DPU. The three components of the magnetic-field vector measured by the Primary Sensor are sampled at a constant rate of 201.93 Hz, independently of the finally transmitted vector rate.

Data acquired at this rate are digitally filtered to match the transmitted rate, according to the operating modes of the instrument (TM option) and the telemetry data rate allocated to it in different spacecraft telemetry modes (TM modes). The telemetry data rates are 1211.13 bits/s, 3465.69 bits/s, 1347.77 bits/s for the 3 Nominal Modes, Burst Mode 1 and Burst Mode 2, respectively. The spacecraft was operated mostly in nominal mode with a primary sensor vector rate of 22.41 Hz and in burst mode with 67.25 Hz.

### 1.3 Instrument overview: EDI

The Electron Drift Instrument (EDI) measures the drift of a weak beam of test electrons, from which the plasma drift velocities can be determined.

We present here a brief introduction into the operational principle of EDI. More details of operation modes and technical characteristics are given in [2], [7] and on: *http://www.mpe.mpg.de/CLUSTER/EDIpages/instr_descrip.html*

The instrument consists of two pairs of electron gun - detector units (GDU). The guns emit weak (≤ 300 nA) beams of 1 keV or 0.5 keV test electrons, in the plane perpendicular to the ambient magnetic field, as measured on board by the FGM and STAFF (Spatio-Temporal Analysis of Field Fluctuations) instruments. Electric fields or magnetic gradients produce a displacement of the beam, after one or more gyrations in the ambient magnetic field. As a result, the beams return to their associated detectors, only when aimed in a unique direction. From the directions the displacement can be determined. For small magnetic fields the triangulation degenerates and the displacement is obtained instead, from the difference in the travel times of the electrons in the two beams.

In order to detect the beam electrons in the presence of background counts from ambient electrons and to measure their flight time, the electron beam is intensity-modulated with a pseudo-noise code (PNC). Correlating the received signal, after a delay corresponding to the time of flight, with the original coded signal, has two important functions. Firstly, correlating the return signal with the emitted signal allows a significant increase in signal-to-background ratio. Secondly, the delay that results in the largest correlated signal corresponds to the time of flight of the electron beam.

The efficiency of EDI is limited by:

1. Magnetic and electric field variability,
2. Signal and signal to background ratio,
3. Accuracy of the real-time on board knowledge of the magnetic field direction.

In this instrument operation mode, called 'windshield-wiper', the telemetric data consist of the electron emission angles, which correspond to the successful detection of the two beams, the two associated electron times-of-flight, plus timing, count-rate and quality information. With the allocated telemetry rate it is possible to transmit this set of measurements every 128 ms in nominal-mode (NM) telemetry and every 16 ms in burst-mode (BM1) telemetry. From the telemetric data one can then derive the drift velocities and the magnetic field strength, in BM1 telemetry and under ideal tracking conditions as often as every 16 ms. It's important to note that the timing of the EDI measurements is not equidistant, i.e. **EDI doesn't produce regularly spaced time series**.

As a by-product, the measured times-of-flight provide an absolute measurement of the magnetic field magnitude (B).The relationship between the electron gyro-time ($T_g$) and the magnetic field strength is:

$$B = 2 \pi m_e/(e T_g), \quad (1)$$

where: $$T_g = (T_1 + T_2)/2 \quad (2)$$

$T_1$ is the time-of-flight (TOF) measured by the first GDU, $T_2$ by the second, $m_e$ and e are the mass and the charge of the electron. T1 and T2 differ from Tg because of the plasma drift velocity, but since one beam is fired "toward" and one "away" from the drift, this cancels in the average [2], [7], [13]. The gyration time of the electrons depends only on the field magnitude and universal constants, such that EDI provides a measurement of the field magnitude in an absolute sense as the scalar magnetometers do, but in a lower field range. The relativistic correction of the electron mass is less than 0.1% for 0.5 and less than 0.2% for 1 keV.

Table 2. Digital resolution of EDI

| B (nT) | Shift-clock Period (μs) | Digital Resolution of B (nT) |
|---|---|---|
| 0 to 15 | 1.907 | 0.012 |
| 16 to 31 | 0.953 | 0.007 to 0.026 |
| 32 to 63 | 0.476 | 0.014 to 0.053 |
| 64 to 127 | 0.238 | 0.027 to 0.11 |
| 128 to 163 | 0.476 | 0.22 to 0.35 |
| 164 to 325 | 0.238 | 0.18 to 0.70 |
| 326 to 657 | 0.119 | 0.35 to 1.4 |

Table 2 shows the digital resolution of the EDI. The time measurement resolution is determined by the shift-clock period. The digital resolution expressed in nT depends on the field strength; since B is inversely proportional to $T_g$, see equation (1).

The two values of the digital resolution converted from the shift-clock periods of column 2 correspond to the lower and upper limits of the magnetic field intervals, listed in column 1.

## 2. MEASUREMENT ERRORS

### 2.1 FGM

The precision of the magnetic field measurement is determined by the digital resolution shown in Table 1 and by the instrument calibration. A brief description of the calibration process for Cluster FGM and of the definition of the parameters that enter into it is given in [1].

Calibration means the determination of parameters that allow the transformation of raw measurements (digitised voltages), as transmitted by the telemetry, in physical units (nT). The transformation of the output of a magnetometer ($\mathbf{B}_M$) to the value of the external field (**B**), to be measured in a reference system, is assumed to depend linearly on the calibration parameters and is expressed mathematically as follows:

$$\mathbf{M}(\mathbf{B}_M - \mathbf{Z}) = \mathbf{B} \quad \Rightarrow \quad \mathbf{R}\,\mathbf{O}\,\mathbf{S}(\mathbf{B}_M - \mathbf{Z}) = \mathbf{B} \quad (3)$$

The matrix **M** with 9 elements was decomposed into three matrices **O, S** and **R** that stay for misalignment, scaling and rotation. Each of these matrices contains three significant elements (besides unity and zero elements). **O** is a triangular matrix, having all principle diagonal elements equal to unity, **S** is a diagonal matrix and **R** is a rotation matrix defining the transformation from the reference system of **B** to the orthogonal sensor system using three Euler angles. **Z** is the vector containing the three components of the sensor offset or zero-level, i.e. the solution for **B** = 0.

Misalignment, scaling and offset errors are combined errors coming from different sources: sensors, electronics and spacecraft background field at the location of the FGM sensor.

Calibration is an iterative process. Ground calibration before launch allows the determination of the parameters of the standalone instrument. Final calibration parameters, including the magnetic influence of the spacecraft on the sensor positions and instrument parameter deviations due to launch stress and specific environment conditions need to be determined in-flight. The calibration has to be repeated because parameters of instrument and spacecraft are variable over time and temperature. In case of Cluster the calibration was done on a daily basis. For higher accuracy special sets of calibration parameters are produced for shorter time intervals.

In case of a spinning spacecraft, like Cluster, in-flight calibration techniques allow the determination of those calibration parameter errors, which produce a spin dependence in the field magnitude time series. The presence of the spin frequency or/and its first harmonic is a sign for poor determination of the spin plane

calibration parameters. The offset and the scale factor, of the spin axis component, are not producing spin dependent signatures and are hence difficult to determine. Some of the techniques applied in special conditions provide the spin-axis offset, however an absolute calibration is possible only with the knowledge of the field magnitude [8]. Statistical calibration methods of vector magnetometers, using as scalar information the field magnitude, are described in [8-12]. They use either model magnetic field magnitude or magnitude information from an absolute (scalar) magnetometer. In our case this information is delivered by EDI.

The flux-gate magnetometer noise is frequency dependent (see Fig.4), such that errors must be specified together with the time interval of their validity. Two sets of error figures are shown in Table 3: one set is valid for 24 hours corresponding to the daily calibration files used in the standard FGM data processing, the other is valid for tens of minutes and is typical for a special calibration file used to produce high resolution data. The differences in the achievable accuracy represent slow changes (drifts) in the instrument parameters. We note also that the figures shown in Table 3 are typical of the magnetometers on all four Cluster spacecraft.

Table 3. Typical FGM measurement errors

| B Range (nT) | sigma_B (nT) | |
|---|---|---|
| | daily calfile | special calfile |
| 0 to 64 | 0.1 | 0.02 |
| 64 to 256 | 0.2 | 0.02 |
| 256 to 1024 | 0.3 | 0.04 |

The measurement errors of Table 3 were obtained by FFT spectral analysis of the magnitude time series, derived from the measured components. They were deduced from the spectral power density at the spin frequencies and characterize thus only the offsets of the spin plane components, the ratio between the spin plane scale values and the three non-orthogonality parameters. The determination of the other parameters: spin axis offset, spin axis scale factor and one of the spin plane scale factors are based on the comparison of the measured magnitude with an independent information on the real magnetic field magnitude. EDI provides this independent information. Since a scaling error is magnitude dependent and the offset not, comparing the measurements at different field strengths can separate them. The differences between the measurements of FGM and EDI were assigned to the spin axis offset in case of Cluster, because no magnitude dependence could be observed. During the commissioning phase of the Cluster experiment, an evaluation of the spacecraft spin axis offset was made and the values (2.45, -1., -2. nT for Cluster 1, 2 and 3, respectively) were determined and introduced in the calibration tables. The comparison with EDI was made, routinely, on a monthly basis, such that the error of the deviation to the absolute magnetic field was about 0.6 nT. Daily or hourly comparisons in order to reduce this error are foreseen. For high-resolution calibration, short time intervals, the error can be made as small as the digital resolution of EDI.

### 2.2 EDI

The precision of the time-of-flight measurement is determined by the time quantization (see Table 2) and the variability of the ambient fields.

In order to cancel out the distortion of the gyration time due to physical effects (drift due to the electric field or magnetic gradient) an average of 2 TOF values measured simultaneously by the 2 GDU's must be used. As the determination of the EDI times of flight by correlation technique is a statistical method, its actual accuracy depends on the flux levels of the returning beam electrons, the flux levels of the ambient electrons in the energy range of the detector and on the variability of the electric and magnetic fields.

In contrast to the FGM errors the EDI measurement errors are not frequency dependent, i.e. they are stable in time up to a frequency of 1 Hz. In order to get this result a FFT analysis of re-sampled EDI time-of-flight measurements was performed. The highest possible frequency for time-equidistant data, starting from burst mode-telemetry was around 1 Hz.

Table 4 gives the limits of some typical all over errors of the EDI magnetic field measurement for best and worst case conditions. Sigma_t is the error of the time-of-flight and sigma_B the corresponding error in B for the maximum field of the range.

Table 4. EDI measurement errors

| B (nT) | sigma_t(μs) | | sigma_B (nT) | |
|---|---|---|---|---|
| | low | high | low | high |
| 10 | 5.4 | 25. | 0.015 | 0.07 |
| 30 | 2.4 | 7.5 | 0.06 | 0.19 |
| 100 | 0.36 | 0.72 | 0.1 | 0.2 |
| 300 | 0.24 | 0.95 | 0.6 | 2.4 |

## 3. COMPARISON OF MEASUREMENTS AND DISCUSSION

Comparison between magnetic field measurements with FGM and EDI were made wherever EDI had good detection efficiency. The detection efficiency is defined as the ratio of the number of spin periods with at least 4 successful measurements per spin to the total number of spin periods. This parameter was computed for 10-minute time-intervals. We computed, for the same time intervals, two parameters: the position of the spacecraft in the magnetosphere and the experimentally determined magnetic field strength. The positions of the spacecraft were determined in geocentric solar ecliptic (GSE) coordinates, in the middle of the time intervals.

The FGM magnetic field data were averaged over the same time intervals in a non-spinning coordinate system and the average magnitudes (B) and the corresponding variances (B_sigma) were computed.

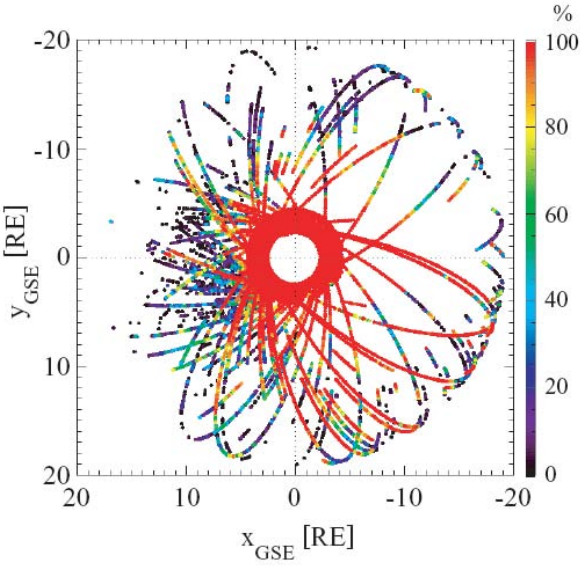


Fig.1 . Map of available EDI magnetic field (TOF) measurements in GSE for Cluster 1,for the time period Feb.2001 - March 2002. The colour bars are scaled by the detection efficiencies: red means 100%.

The available EDI magnetic field (TOF) measurements for Cluster 1, over the period February 2001 - March 2002, mapped in the GSE x – y plane, is shown in Fig. 1. The colour bars are scaled with the detection efficiency values; red means 100% detection efficiency. The predominance of red close to perigee suggests a preference of EDI for stronger magnetic fields.

The dependence of the EDI detection efficiency on the magnetic field properties is shown in Fig. 2. In the upper panel (Fig. 2a), the efficiencies are plotted against the magnetic field magnitude (B) and local time (derived from the spacecraft position expressed in GSE spherical coordinates) for the same period and spacecraft. The preference for strong fields is obvious. An increased EDI efficiency in the lower field limit for late local times (18 – 24 hours) suggests a relation to the magnetic field variability, which is lower in the flanks and the tail of the magnetosphere, than close to the bowshock, for the same field strength. The dependency on the magnitude and variance of the magnetic field is shown in the lower panel (Fig. 2b). B_sigma is the normalized variance of the total magnetic field and has the following expression:

$$\mathbf{(<B \bullet B> - <B> \bullet <B>) / <B \bullet B>} \qquad (4)$$

where < > stands for averaging and **B•B** is the scalar product.

The limitation of low fields and high variability is clearly visible in Fig. 2b. The two drastic changes in the values of B_sigma, around 80, respectively 260 nT, are related to the different digital resolution of FGM in the three used ranges (see Table 1).

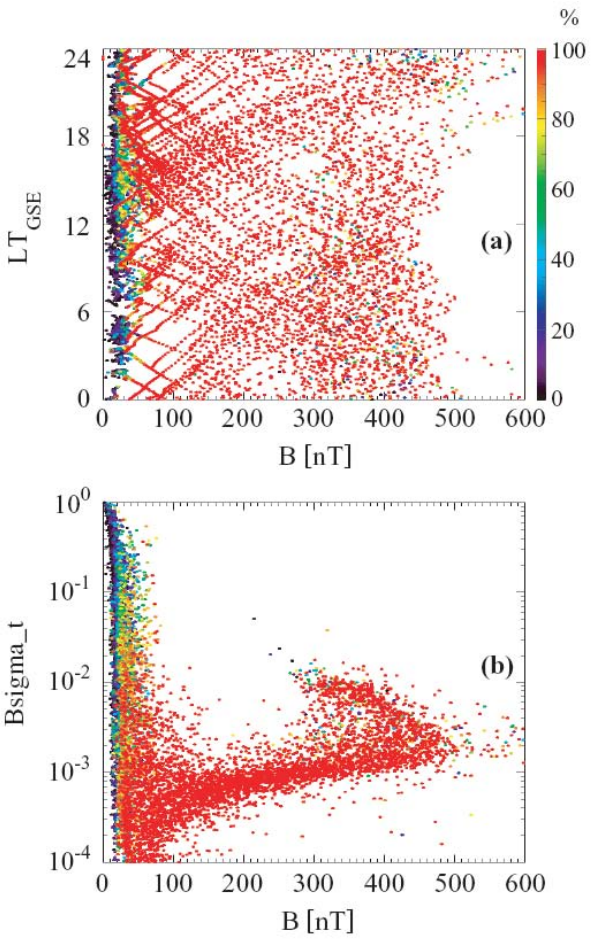


Fig.2. EDI detection efficiencies (%) versus FGM magnetic field (nT) for Cluster 1 and GSE local-time (upper panel) or FGM magnetic field variance (lower panel)

Two typical examples of magnetic field data measured by FGM and EDI in different ranges and TM modes are shown in Fig.3. They were selected randomly from the data, one from nominal mode, and the other from burst mode.

The magnetic field magnitudes are in the 400 nT and 40 nT ranges, which correspond to different magnetospheric regions: cusp and tail. In the first case the spacecraft crosses the southern cusp close to perigee (Fig. 3a). The depression in the field, which otherwise would show a maximum at perigee, is due to the cusp. The second example shows a tail crossing close to apogee. The spacecraft is slowly drifting away from the equatorial plane at around 22h local time and the magnetic field is quasi-uniform.

The data were transmitted in burst, respectively nominal telemetry modes. The blue points are high resolution EDI time-of-flight data converted into magnetic field magnitude, the red points are statistically reduced data points to the limit of the digital resolution and the black line is the high resolution, respectively spin averaged, magnetic field as measured by FGM.

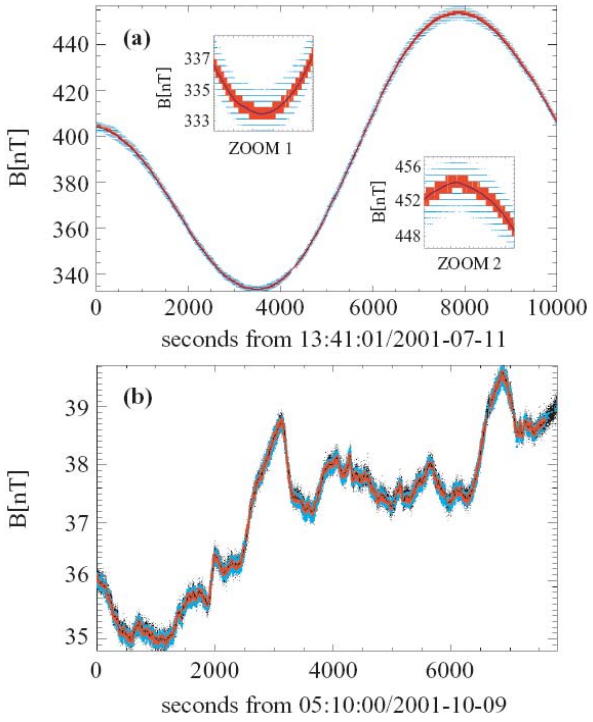


Fig.3. Magnetic field magnitude by FGM (black line) and EDI using TOF measurements (blue points for the raw data and red lines for the selected data) in the: (a) 400 nT range, data form Cluster 1 (Rumba) - upper panel and (b) 40 nT range data from Cluster 3 (Samba) - lower panel..The two zoom figures in Figure 3(a) are each 1000-second long.

The digital resolution of the time-of-flight measurement is visible in the vertical layering of the EDI high resolution data-points in the zoom. In order to compare two fundamentally different instruments we had to characterize their performances in similar ways. Since the paper investigates the ability of EDI to measure the magnetic field, it seemed appropriate to apply magnetometer parameter definitions to EDI.

The frequency dependence of the FGM noise (in pT/√Hz) is presented Fig. 4. It is typical for flux-gate magnetometers and is independent of the value of the magnetic field for low frequencies. The range dependence becomes apparent at higher frequencies. To illustrate the full range of the frequency response of FGM, the noise values of the lower frequency end (< 0.01 Hz) were taken from measurements made on similar flux-gate magnetometers produced by MAGSON Gmbh for magnetic observatories. Similar means here: having the same noise level at 1 Hz.

The power spectral density for EDI in μs/√Hz, was obtained by making a FFT transform of a resampled time series of gyro-times. No frequency dependence was observed. A line was fitted to the data and transformed into pT/√Hz for two magnetic field strength values. The resulting two lines are shown in Fig.4.

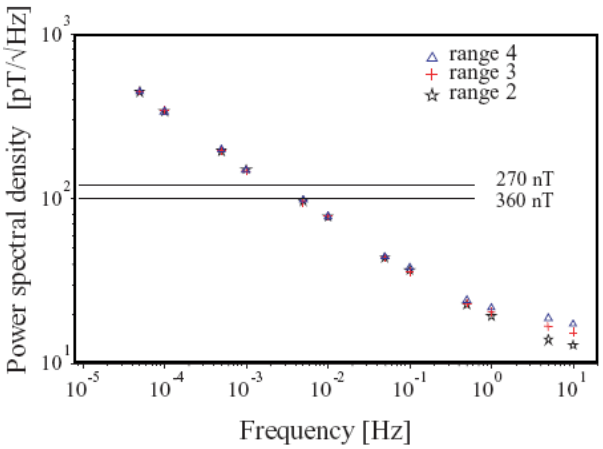


Fig.4. The frequency dependence of instrument noise in three FGM-ranges.The symbols star, cross and triangle stand for ranges 2,3 and 4, respectively. Differences are visible only in the high frequency region. The lines resulted from a least squares fit to EDI power spectral density for 360 and 270 nT

The intercept between the FGM and EDI curves shifts toward lower frequencies with decreasing field strength. We distinguish 2 intervals: one of high frequency where the EDI error predominates and another for very low frequencies where the magnetometer instrument noise predominates. A spin-axis offset determination using EDI makes sense only in the frequency interval where EDI errors are smaller than the FGM ones. That means that a smaller than hourly interval for calibration using EDI is not recommended.

FGM and EDI measurements have been compared systematically from the beginning of the Cluster mission. Initially, EDI measurements were used to improve the in-flight calibration of the magnetometers; in the later, operational phases of the mission, the comparison has been used to check and validate the calibration parameters of the magnetic field. The comparison is performed as follows:

1. EDI time-of-flight data are converted into magnetic field magnitude,
2. High resolution calibrated FGM magnetic field vectors are computed in spacecraft coordinate system,
3. A fit of the FGM magnetic field magnitude to the EDI magnetic field magnitude is performed, using the offsets as free parameters and the field components as independent variables.

4. The resulting offsets for each range and spacecraft are added to monthly survey tables. The survey tables are then used to adjust, if necessary, the spin axis offsets in the daily calibration tables.

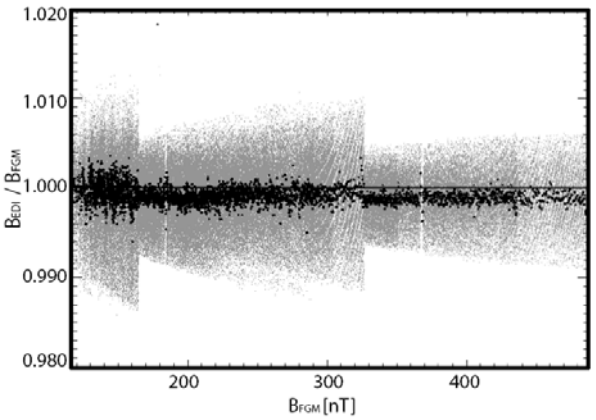


Fig.5. The ratio of B_EDI and B_FGM, versus B_FGM is shown for 12 hours of data from December 2002 days (2, 5, 9, 12, 21, 24, 28, 31).

To get a statistical overview on the comparison of the 2 instruments, we selected 12 hours of high-efficiency EDI data and plotted the ratio between the magnetic field magnitudes measured by EDI and FGM versus B_FGM. The data are from Cluster 2 spacecraft, days: 2, 5, 9, 12, 21, 24, 28, 31 of December 2002 (Fig. 5). The two jumps in the data spread of the raw data correspond to the changes in the EDI digital resolution (see Table 2). The light-grey points are ratios of EDI raw data to FGM interpolated at the same time moments. The black points are ratios of 8-second averages. Daily calibration files were used to process the FGM data. The absolute error of the magnetic field measurement is close to 0.1 nT for fields below 100 nT and less than 0.1% for fields above.

## 4. CONCLUSION

Systematic comparison of the magnetic field measurements by the FGM and EDI instruments on the four-spacecraft Cluster mission has been used to determine spacecraft offsets and offset changes and to improve the calibration and validation of the magnetic field vector measurements made by FGM. The ability of the EDI instrument to measure the absolute value of the magnetic field has provided a rare opportunity to make an absolute calibration of a flux-gate magnetometer in-flight, similarly to scalar calibration by means of a proton magnetometer. The paper shows that the consequent FGM-EDI comparison of the magnetic field magnitude, on daily basis, guaranties accuracy better than 0.1% for the Cluster magnetic field measurement. The full resolution time-of-flight data from EDI, part of the Cluster Active Archive [13], allows to get the best possible calibration for the higher than spin-resolution FGM data.

**References**

[1] Balogh, A. et al, "The Cluster Magnetic Field Investigation:Overview of in-flight performance and initial results", *Ann.Geophys*., Vol.19, No.10-12, page 1207 - 1217, 2001

[2] Paschmann, G. et al, "The Electron Drift Instrument on Cluster: Overview of First Results", *Ann.Geophys*., Vol.19, No.10-12, page 1273 - 1288, 2001

[3] Reigber, Ch., Luehr, H. and Schwintzer, P., "CHAMP Mission Status", *Advances in Space Research*, Vol. 30, No. 2, pp. 129-134, 2002

[4] Olsen, N. et al., "Calibration of the Oersted vector magnetometer", *Earth Planets Space*, 55, 11-18, 2003).

[5] Fornacon, K.-H. et al, "The magnetic field experiment onboard Equator-S and its scientific possibilities", *Ann. Geophysicae* Vol.17, 1521-7, 1999

[6] Paschmann, G. et al, "EDI electron time-of-flight measurements on Equator-S", *Ann. Geophysicae* Vol. 17, 1513-1520, 1999

[7] Vaith, H. et al, "Electron Gyro Time Measurement Technique for Determining Electric and Magnetic Fields", in *Measurement Techniques in Space Plasmas, Fields*, *Geophysical Monograph* 103,Page 47 – 52, 1998.

[8] Auster, H.U. et al, "Calibration of flux-gate magnetometers using relative motion", *Meas.Sci.Technol*., Vol.13, page 1 - 8, 2002

[9] Wertz, J.R., *Spacecraft Attitude Determination and Control*, Kluwer Academic Publishers, Dordrecht/Boston/London, 1978, page 329

[10] Davis, L. und E.J.Smith, "The inflight determination of spacecraft field zeros", *Eos Trans., AGU, 49, 257*, 1968

[11] Lerner, G. M. und M. D. Shuster, "Magnetometer Bias Determination and Attitude Determination for Near-Earth Spacecraft", *J.GUID.CONTROL* 4: 518-22, 1981.

[12] Merayo, J.M.G., et al., "Scalar calibration of vector magnetometers", *Meas. Sci. Technol*., Vol. **11,** 2000, page 120-132.

[13] Georgescu, E. et al., "Archiving of the Cluster EDI data", this volume